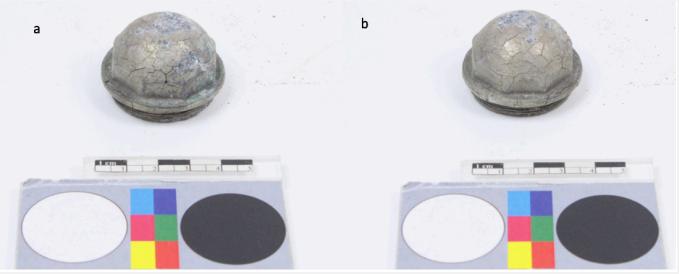
DOMED CAP NUT - ZN AL SN CU ALLOY - MODERN TIMES - FRANCE

Artefact name	Domed cap nut
Authors	Christian. Degrigny (HE-Arc CR, Neuchâtel, Neuchâtel, Switzerland) & Mathea. Hovind (University of Oslo, Department of archaeology, conservation and history (IAKH-UiO), Oslo, Oslo, Norway)
Url	/artefacts/402/

The object



Credit UiO-IAKH, M.Hovind.

Fig. 1: Domed, threaded fitting, consisting of a Zn/Al/Pb/Cu/Sn alloy. Profile «a» and «b», to the left and right, respectively,

Description and visual observation

Description of the artefact	A domed, threaded fitting, consisting of a cast alloy with a metallic plating (Fig. 1). Its shape is octagonal and the inside is hollow. The plating is heavily cracked, leading to surface flaking. The metal appears to be consumed by some kind of internal corrosion. Dimensions: L (ø) = 40mm; H = 28mm; T = 5mm; WT = 49g.
Type of artefact	Cap
Origin	Château de Germolles, Mellecey, Bourgogne, France
Recovering date	Date unknown
Chronology category	Modern Times
chronology tpq	1801 A.D.
chronology taq	2000 A.D.
Chronology comment	19th - 20th century
Burial conditions / environment	Outdoor atmosphere

This work is licensed under CC BY-NC-ND 4.0

Artefact location	Haute Ecole Arc Conservation-Restauration
Owner	Château de Germolles, Mellecey, Bourgogne
Inv. number	Not registered.
Recorded conservation data	No conservation data recorded.

Complementary information

Nothing to report.

Study area(s)

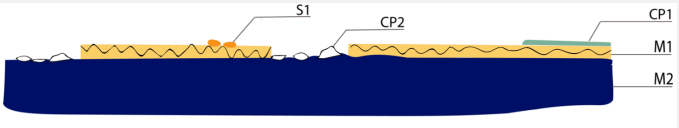


Credit UiO-IAKH, M.Hovind.

Fig. 2: Zones of the artefact submitted to visual observation and location of sampling area (a cross-section of the metal marked by the stippled line),

Binocular observation and representation of the corrosion structure

The schematic representation below (Fig. 3) gives an overview of the corrosion layers encountered on the object from a first visual macroscopic observation.



Captions	Description
S1	Localized bright orange spots. Possibly exogenous in origin (from Fe-rich soil).
CP1	Thin, translucent, green layer with scattered distribution. Mainly located towards the bottom part of the fitting (right above the threads).
M1	Cracked metal plating with a submetallic golden sheen.
CP2	White, powdery and isolated corrosion product. Mainly located where the bare metal is left exposed.
M2	Intact metal, appearing grey-blue in colour. In areas where the metal plating (M1) has broken, the metal protrudes above the original surface and is covered by a white powdery corrosion product (CP2).

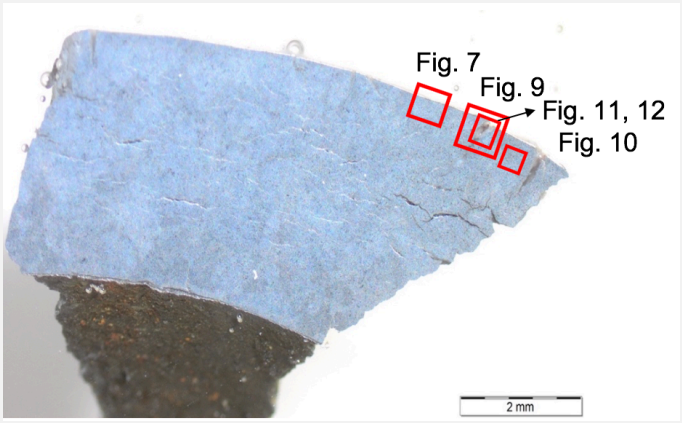
Credit UiO-IAKH, M.Hovind

Fig. 3: Preliminary stratigraphy corresponding to the overall surface of the artefact. CP = Corrosion Product, S = Soil, M = Metal,

This work is licensed under CC BY-NC-ND 4.0

MiCorr stratigraphy(ies) – Bi

Sample(s)



Credit UiO-IAKH, M.Hovind.

Fig. 4: Micrograph of the cross-section showing the locations of Figs. 7 and 9-12,

Description of sample	The sample is a cross section of the metal, representative of the head of the fitting. It shows external cracks extending from the metal surface and into its structure in addition to internal cracks, visible as thin lines along its longitudinal axis (Fig. 4).
Alloy	Zn Al Sn Cu Alloy
Technology	None
Lab number of sample	NZC2018 (Ni/Zn Cap, sampled in 2018)
Sample location	HE-Arc CR, Neuchâtel, Neuchâtel
Responsible institution	Haute Ecole Arc Conservation-Restauration
Date and aim of sampling	March 2018, study of corrosion stratigraphy and chemical analyses

Complementary information

The fact that the artefact was considered as test material enabled extensive sampling that would not otherwise be possible.

Analyses and results

Metallography

Microscope: Leica DMi8 (a metallographic, inverted, reflected light microscope) with magnification up to 500X.
Camera: Olympus SC50 connected to the software "Olympus Stream", version 1.9.4. Illumination modes: bright field and cross-polarized light.

SEM-EDS

Instrument: Jeol 6400; voltage: 20 kV; working distance: 18 and 24mm; sample preparation: palladium depot.

This work is licensed under CC BY-NC-ND 4.0

Non invasive analysis

Metal

The metal of the domed fitting (M2) consists of a Zn/Al/Pb/Cu/Sn alloy (Table 1) externally covered by a nickel-based plating (M1) (Figs. 7 and 8). The bulk metal (M2) has a dendritic microstructure appearing light grey in bright field, while the interdendritic phase appears white (Fig. 9). The latter is Zn-rich, while the dendritic phase consists of approximately equal amounts of Zn and Al (Table 2, Fig. 11). Observation in SEM (BSE-mode) reveals the presence of Pb-nodules, visible as white irregular spots with a scattered distribution, in addition to opaque grey patches which are rich in Al and Fe (Fig. 10).

Elements	Zn	Al	O	C	Pb	Cu	Sn	Si	Fe
mass%*	54	23	11	6	3	2	1.5	0.3	0.2

Table 1: Chemical composition of the metal (M2). Method of analysis: SEM-EDS. Lab. of Electronic Microscopy and Microanalysis, Néode, HEI Arc, credit MiCorr_HEI Arc, C.Csefalvay. *The value is the calculated average of three analyses of the same feature, but in different areas.

Elements Mass%*	Zn	Al	O	C	Pb	Cu	Sn	Si	Fe
Dendrites	31	32	25	6	2	2	1	0.2	0.1
Interdendritic phase	86	0.7	2	6	3	2	0.8	0.2	0.1

Table 2: Chemical composition of the matrix consisting of dendrites and an interdendritic phase. Method of analysis: SEM-EDS. Lab. of Electronic Microscopy and Microanalysis, Néode, HEI Arc, credit MiCorr_HEI Arc, C.Csefalvay. *The value is the calculated average of three analyses of the same feature, but in different areas.

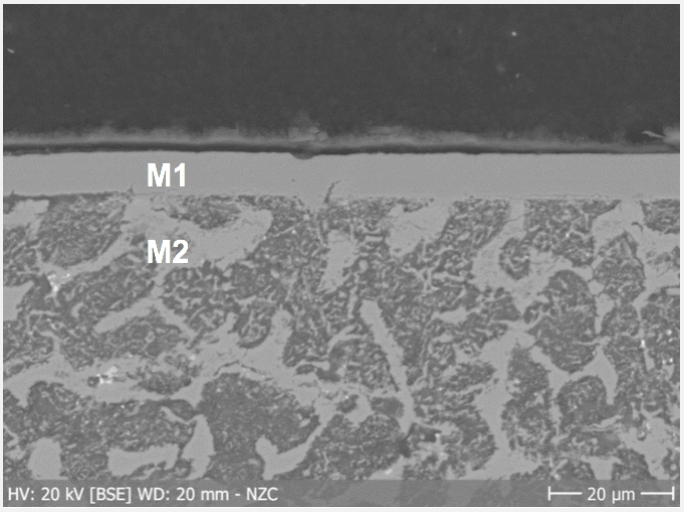
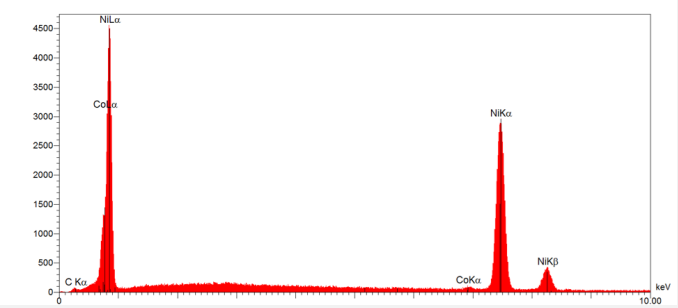


Fig. 7: SEM-image (BSE-mode) of a selected area from Fig. 4 (detail), showing the metal plating (M1) and the bulk metal (M2),

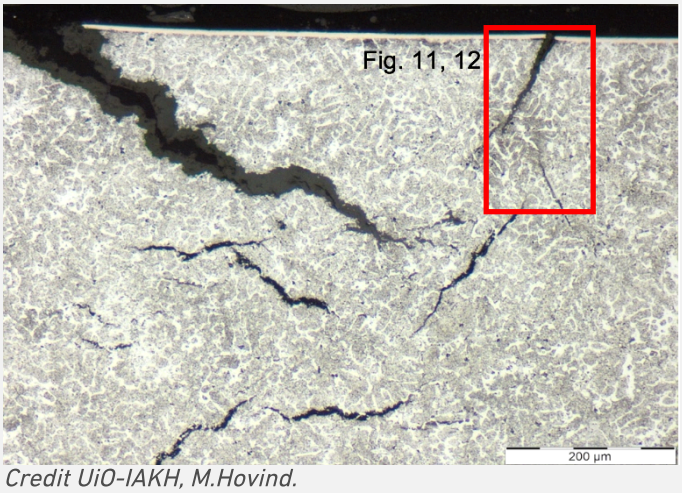
This work is licensed under CC BY-NC-ND 4.0

Credit HEI Arc, C.Csefalvay.



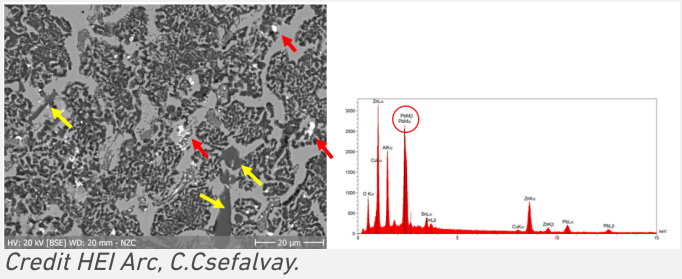
Credit HEI Arc, C.Csefalvay.

Fig. 8: EDS-spectrum showing the chemical composition of the metal plating (M1). Method of analysis: SEM-EDS. Lab. of Electronic Microscopy and and Microanalysis, Néode, HEI Arc,



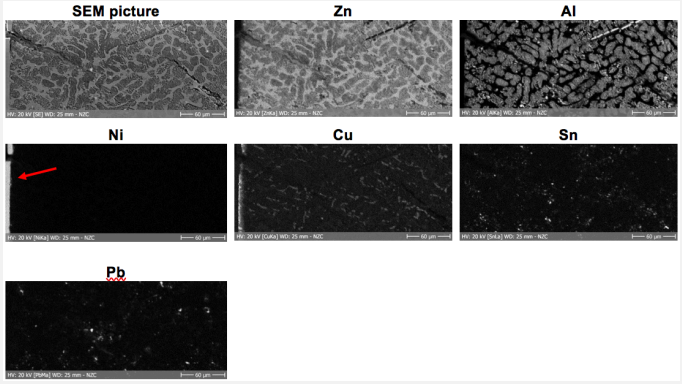
Credit UiO-IAKH, M.Hovind.

Fig. 9: Micrograph of the metal sample from Fig. 4 (detail), unetched, bright field. The dendrites appear light to dark grey while the interdendritic phase appears white. The metal is characterized by surface cracks as well as internal cracks. The upper red square corresponds to the area selected for elementary mapping by SEM-EDS (Figs. 11 and 12),



Credit HEI Arc, C.Csefalvay.

Fig. 10: SEM-image in BSE-mode (left) and EDS-spectrum (right), showing the appearance and the chemical composition of the Pb inclusions (red arrrows). The inclusions appear white, the dendrites appear dark grey/black and the interdentritic phase appears grey. Grey opaque patches (yellow arrows) are Fe- and Al-rich phases,



Credit HEI Arc, C.Csefalvay.

Fig. 11: SEM image and elemental chemical distribution of the selected area from Fig. 9 (rotated 270° and inversed). Method of analysis: SEM-EDS. Lab. of Electronic Microscopy and Microanalysis, Néode, HEI Arc,

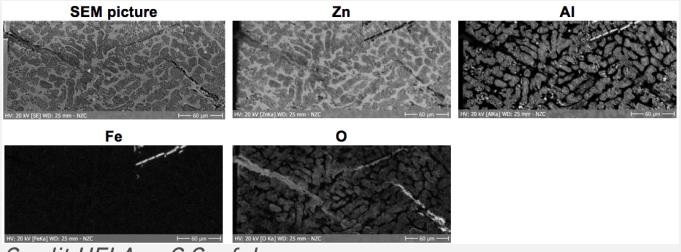
Microstructure	Dendritic structure
First metal element	Zn
Other metal elements	Cu, Sn, Pb, Al

This work is licensed under CC BY-NC-ND 4.0

Corrosion layers

The dendritic phase is heavily oxidized compared to the interdendritic phase (Table 2 and Fig. 12). The corrosion has developed throughout the entire metal body, generating cracks (Fig. 9). The cracks are Zn and O-rich (Fig. 12) and could be composed of zinc carbonate. It could be a case of zinc pest, an intergranular corrosion phenomenon known to cause disintegration in poor quality alloys (Selwyn 2004:155-156, Zhang 2011:890).

The external corrosion products and deposits (Fig. 3) were documented but not analyzed as they were considered to be mainly exogenous in origin and not the main reason behind the deterioration of the object. The orange deposit (S1) is probably soil from Fe-rich environment, while the thin green layer (CP1) is most likely consisting of an oxide of Ni from the metal plating (M1). The white corrosion product (CP2) can either be a salt from the environment, or corrosion products of Zn/Al.



Credit HEI Arc, C.Csefalvay.

Fig. 12: SEM image and elemental chemical distribution of the selected area from Fig. 9 (rotated 270° and inversed). Method of analysis: SEM-EDS. Lab. of Electronic Microscopy and Microanalysis, Néode, HEI Arc,

Corrosion form	Internal cracking
Corrosion type	zinc pest

Complementary information

Nothing to report.

MiCorr stratigraphy(ies) – CS

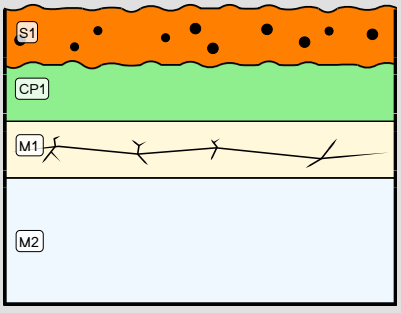


Fig. 5: A MiCorr stratigraphy representative of an area with intact metal plating (M1). S1 represents Fe-polluted soil while CP1 is a green translucent corrosion product, Credit UiO-IAKH, M.Hovind.

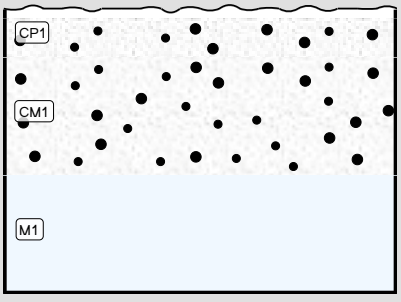
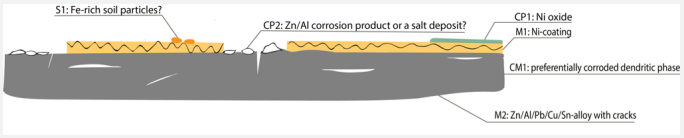


Fig. 6: A MiCorr stratigraphy representative of an area where the metal plating is missing. CP1 corresponds to CP2 in Fig. 3, CM1 represents the corroded metal phase, while M1 corresponds to the bulk metal (M2 in Fig. 3), Credit UiO-IAKH, M.Hovind.

This work is licensed under CC BY-NC-ND 4.0

Synthesis of the binocular / cross-section examination of the corrosion structure

Nothing to report.



Credit UiO-IAKH, M.Hovind.

Fig. 13: Corrected stratigraphic representation with results from SEM-EDS analysis and visual microscopic observation. The colour of the metal was changed to grey as this was the colour of the metal when viewed in cross-section. CP = corrosion product, S = soil, M = metal, CM = corroded metal,

Conclusion

The domed, threated fitting consists of a Zn/Al/Pb/Cu/Sn alloy with a Ni-based plating. It has a dendritic microstructure, indicative of production by casting (probably a die cast). The deterioration of the metal could be due to absence of cohesion between the different phases which enabled the penetration of oxygen during the manufacture of the alloy and the formation of internal corrosion products, eventually leading to expansion of its internal structure (zinc pest).

References

References sample:

1. Selwyn, L. (2004). Metals and corrosion: A handbook for the conservation professional. Ottawa: Canadian Conservation Institute.

2. Zhang, X. G. (2011) “Zinc”. In. Revie R. W. ed. Uhlig’s Corrosion Handbook, 3rd ed. Toronto, ON: John Wiley & Sons, p. 879 – 892.

This work is licensed under CC BY-NC-ND 4.0